Multi-domain approach to modeling pantograph-catenary interaction

Indexed by:
Web of Science Group

Paweł Zdziebko[a,*], Adam Martowicz[a], Tadeusz Uhl[a]

[a] AGH University of Science and Technology, Faculty of Mechanical Engineering and Robotics, Department of Robotics and Mechatronics, al. A. Mickiewicza 30, 30-059 Krakow, Poland

Highlights

- Multi-domain simulation for a pantograph-catenary system has been proposed.

- Analysis of importance of physical domains included in the model has been performed.

- Aerodynamics has been identified as the most influential domain in the model.

- It has been shown that the electromagnetic induction force can be neglected.

Abstract

When a railway pantograph interacts with a catenary during the movement of a rail vehicle, several physical phenomena, both mechanical and electrical, occur in the system. These phenomena affect the quality of power supply of a train from traction devices. The unfavourable arcing occurring when there are disturbances of contact between the pantograph's slider and the catenary contact wire. In turn, it results in energy loss and increased wear of the components of the system. When designing new solutions, computational models are helpful to predict the quality of interaction between the components of the pantograph-contact line system already at the virtual prototyping stage. In this paper, the authors comprehensively present a multi-domain (multiphysics) model, which takes into account necessary conditions for interaction between pantograph elements and a catenary. Finally, the impact of the individual physical domains are analysed and the ones which have a significant impact on the simulation of the operation results are identified.

Keywords

pantograph-catenary system, dynamic interaction, multi-domain approach, numerical simulation, Finite Element Analysis, multibody dynamics, co-simulation.

1. Introduction

The pantograph mechanism is used for receiving electrical power from a catenary. It is used in trams, freight locomotives, and high-speed passenger trains. A typical 160ECT [10] pantograph is presented in Figure 1. When interacting with a catenary, a collector head with carbon strips is in a sliding contact with a catenary contact wire. The electrical power is transferred through the pantograph structural elements (arms, links and frame), and then to the electrical system of the rail vehicle.

Increases in trains speeds are observed for years and require improvements to the various components of the whole system, covering both vehicles and the entire infrastructure. Due to the proportional relationship between the train speed and the current consumed from the traction system, the mechanisms for collecting power from the catenary is one of the factors limiting the maximum speed of trains. Figure 2A presents the main components of the catenary system.
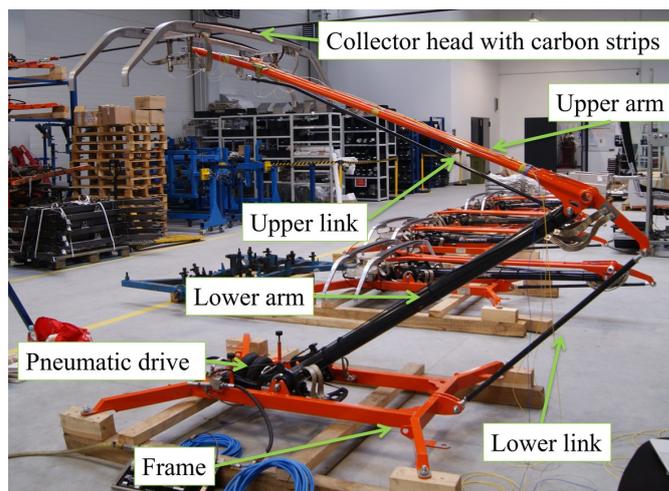

Fig. 1. Pantograph mechanism on a test stand

(*) Corresponding author.
E-mail addresses: P. Zdziebko (ORCID: 0000-0001-6845-033X): zdziebko@agh.edu.pl,
A. Martowicz (ORCID: 0000-0001-9630-0355): adam.martowicz@agh.edu.pl, T. Uhl (ORCID: 0000-0002-4332-3067): tuhl@agh.edu.pl
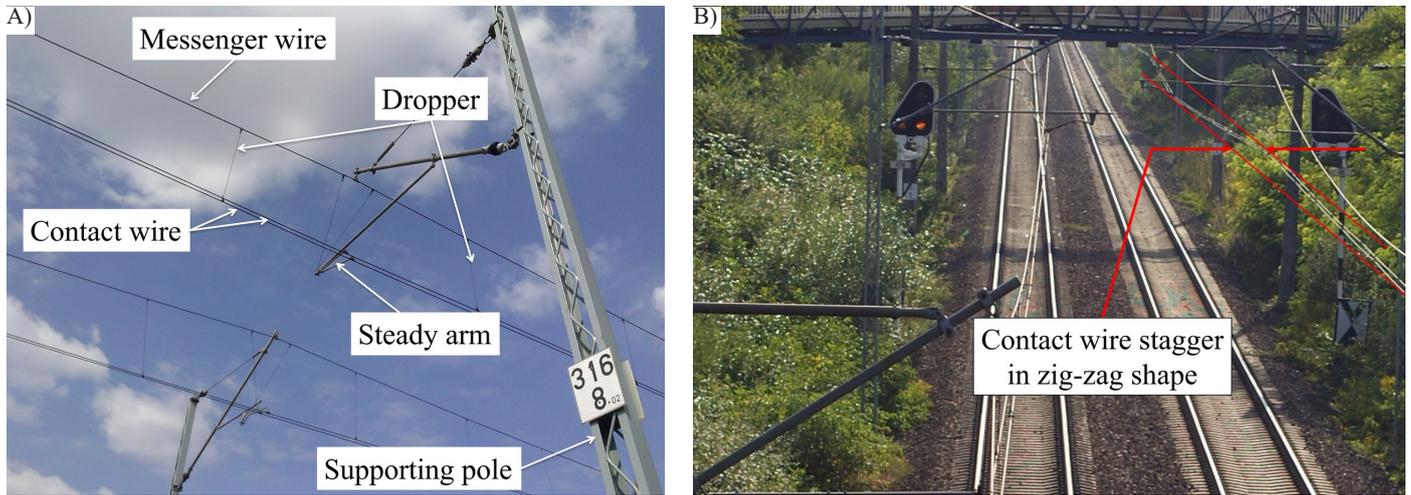
Fig. 2. Description of the catenary system: (A) components of the catenary system and (B) catenary staggering – photographs taken by Pawel Zdziebko

The catenary is a flexible, periodic structure which consists of a contact wire and a messenger wire. The messenger wire is suspended to the poles with supporting arms, while the contact wire is suspended to a messenger wire using droppers and steady arms. On straight track sections, the catenary is staggered as shown in Figure 2B. This makes the pantograph slider wear evenly when travelling over long straight sections, because the contact point keeps moving from side to side of slider. Contact and messenger wires are subjected to tension, which reduces the unevenness of the stiffness of the catenary. Railway power supply systems are considered to be critical in terms of reliability, it is also postulated that they should be treated as critical for safety [24]. At high speeds, fluctuations in contact force (CF) are observed. They may lead to a loss of contact between the pantograph head and the contact wire. Even small disturbances in contact, lasting a few milliseconds, may cause arcing in the contact area. This results in the increased wear on the components, that remain in contact, due to heating and melting the materials. Thermal wear is one of the important factors limiting the lifetime of the pantograph slider and reliability of the system [9]. Increased wear of contact strips increase the risk of fatal failure in pantograph-catenary interaction. In the recent paper [17] authors emphasize that very strict monitoring of contact strips is extremely important, because its timely replacement guarantees trouble-free operation and no need for costly and long-lasting repairs. The authors proposed an evaluation method of preventive renewal strategies of railway vehicles selected parts, which has been demonstrated for contact strips case study . The research on thermal and mechanical wear of the contact wire and pantograph head strip [3, 5, 23] shows that the increased uplift force between the pantograph and the traction reduces arcing, but at the same time, increased sliding friction force increases mechanical wear. Pombo et al. [27] concludes that the use of two pantographs on a single rail vehicle significantly influences fluctuations in CF. However, with appropriately adjusted pantograph spacing, such a configuration may improve dynamic interaction with the catenary[18]. The latest studies also indicate the significant impact of the rail vehicle on the resulting quality of the interaction between the pantograph and the catenary. The research conducted by Song et al. [30] shows that poor track quality reduces the quality of the pantograph's interaction with the catenary.

The numerical models of dynamic interaction between the catenary and pantograph are commonly used for designing the system components. Moreover, the Technical Specifications for Interoperability (TSIs) issued by the European Commission require the presentation of numerical results for positive certification process of the pantographs and overhead contact lines components. Those documents define the technical and operational standards which must be met by the pantograph-catenary system components in order to meet requirements and ensure the interoperability of the railway systems.

The simplest computational models for simulating the interaction between the pantograph and the catenary with the lumped parameters date back to the 1970s [13, 14]. Models with one [31, 32] or more [26, 28] degrees of freedom (DOFs) are based on a variable stiffness representing the catenary system. A small number of DOFs results in high computational performance for these models. Above mentioned elementary models provide an overall understanding of the interaction between the pantograph and the catenary, but they still exhibit several imperfections. The most important ones are the mechanical wave propagation in the overhead contact line being overlooked, followed by significant oversimplification of the pantograph model. These drawbacks result in a failure to properly validate these models according to the applicable EN 50318 standard [11]. Application of the Finite Element Method (FEM) in the catenary model allows one to account for propagation and reflection of the mechanical wave [15] on the overhead contact line and the nonlinear characteristics of the droppers. Such improvements allowed one to obtain a positive validation results against the EN 50318, as published by Carnicero et al. [4].

Simplified pantograph models with lumped parameters are being replaced by the Multibody Dynamics (MBD) models, as demonstrated, by Ambrosio et al.[2], Pappalardo et al. [25], and Song et al. [29]. In these models, rigid pantograph components, described by geometry, material, and inertial properties, are interconnected using rotating and sliding kinematic pairs. To enable simulations using the FEM model of the overhead contact line and the advanced MBD pantograph model, it is necessary to use the co-simulation procedure as shown in work by Massat et al. [20] and Ambrosio et al. [1]. This algorithm relies on exchanging data between the pantograph and catenary models during the simulation. This approach allows to simultaneously take advantage of the FEM model of the catenary and the MBD model of the pantograph. Simulations based on co-simulation procedure are currently the most advanced method for numerically testing the pantograph-catenary system.

Despite the computational models used being highly sophisticated, it should be highlighted that there is still a need to improve them. The model that would simultaneously take into account the effects of all relevant forces and torques which are affecting pantograph-catenary interaction is needed. The authors' review showed that the models reported in the literature usually ignore such phenomena as the effects of aerodynamic forces, electromagnetic forces, or rail vehicle dynamics. Moreover, it is not clearly defined which phenomena are necessary in modelling and which can be ignored due to the small influence on the obtained results of numerical simulations. In response to the imperfections of existing models, in this paper, we use a multi-domain approach for analysing the interaction of the pantograph and catenary. The purpose of the works presented herein is to build a multi-domain numerical model describing the behaviour of the

overhead contact line and pantograph system including all potentially important factors. Another goal is to investigate effect of their omission in the multi-domain simulation model and propose guidelines for pantograph-catenary modelling process in this field.

This paper consists of the following parts: In Section 2, we present the proposed multi-domain model of the catenary-pantograph system. Section 3 describes the details of the FEM model of the catenary, including the shape-finding methodology and validation results for this model. Next, Section 4 presents the details of the MBD pantograph and rail vehicle model. Section 5 presents the simulation results for the tested 160ECT pantograph. This Section also investigates the influence of individual phenomena omission on the results of the multi-domain model simulation. Finally, conclusions are presented in Section 6.

2. Multi-domain simulation of a pantograph-catenary system

As already mentioned in the literature review in Section 1, there is still a need to develop computer modelling and simulation techniques for the pantograph-catenary system. Such a model should be considered as multi-domain system, because the resulting interaction between the pantograph with the catenary is affected by various phenomena. In the paper, we present the methodology for conducting computer simulations for a multi-domain model of pantograph and catenary. The system under consideration has been presented schematically in Figure 3.
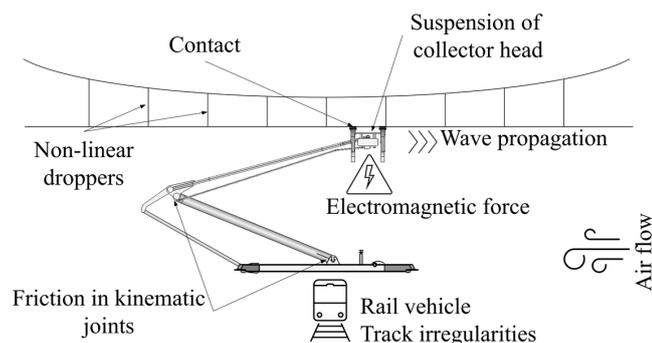

Fig. 3. Physical phenomena in the pantograph-catenary interface

Figure 3 shows schematically important phenomena that can have a key impact on the quality of the interaction between the pantograph and the overhead contact line. In the proposed numerical model, the following are taken into account:

- Three-dimensional pantograph model, which reflects a kinematic chain of the mechanism, with friction model in kinematic joints.
- Model of the rail vehicle together with track irregularities which causes vibration of the vehicle body, and then, vibration of the pantograph frame.
- Aerodynamic and electromagnetic forces, which acts on the pantograph components and influence the pantograph uplift force.

- Nonlinearities of the catenary system, resulting from the non-linear stiffness of droppers and relatively large displacements of cables.
- The phenomenon of mechanical wave propagation in the overhead lines during the passage of the pantograph and rail vehicle.

For the studies presented in this paper, we assumed a straight-line section of a track and catenary. The pantograph mechanism is located on the roof of the rail vehicle. Due to the specificity of the modelled system, it is necessary to describe interactions between its components with significantly different stiffness properties. Therefore, we used the MBD approach for modelling the pantograph and the rail vehicle. The rail vehicle travels on tracks described using the vertical irregularities profile for each rail independently. The pantograph's kinematic joints are modelled with dry sliding friction. The proposed pantograph model also takes into account the impact of aerodynamic forces. They have a significant effect on the CF when travelling at high speed. The electromagnetic force, induced by the current conducted through the catenary and the pantograph head, has also been taken into account. We modelled the flexible catenary system using the FEM and took into account propagation and reflection of the mechanical wave in its structure. The catenary model accounts for the non-linear nature of the droppers which are made of a steel cable that remains stiff under tensile stress but is elastic in compression.

Figure 4 presents a diagram with computer simulations proposed herein. The proposed approach to simulating pantograph interaction with traction is based on integrated FEM-MBD model, and thus the model shall be treated as coupled. The data exchange between these partial models is carried out using the co-simulation procedure. First, sub-models are formulated to determine the pre-configuration of the catenary and calculate the electromagnetic and aerodynamic forces acting on the pantograph components. These models are later described in the paper. At the same time, other relevant parameters of the rail vehicle and pantograph model are defined, such as the speed of the rail vehicle, the profile of the vertical track irregularities, the coefficient of friction in the pantograph kinematic pairs, the nominal uplift torque of the pantograph (responsible for the static uplift force of the pantograph slider), and the suspension parameters of the pantograph slider. Next, the dynamic interaction between pantograph and catenary using co-simulation is lunched. The procedure is based on data exchange in subsequent calculation steps between FEM (catenary) and MBD (pantograph-rail vehicle assembly) models. In order to ensure high quality of the FEM and MBD models, validation of
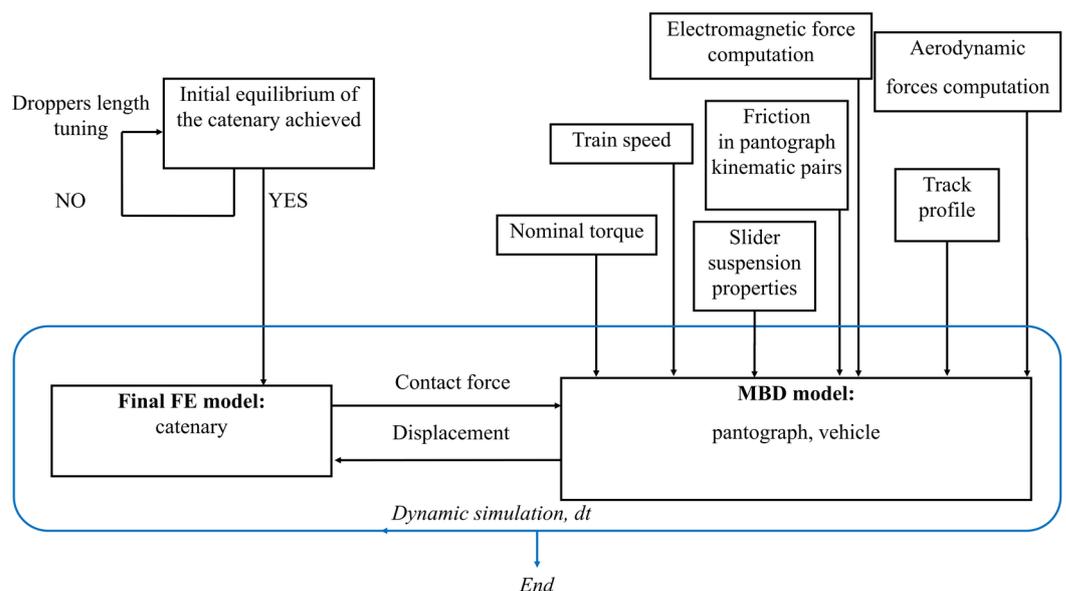

Fig. 4. The proposed multi-domain approach for pantograph-catenary simulation

selected sub-models is needed to be carried out (to the extent available to conduct). The catenary model is validated against the EN 50318, while the MBD pantograph model is formulated based on the technical data provided by the manufacturer, and therefore is assumed to be realistic. Collector head suspension properties, friction in kinematic joints and aerodynamic properties were identified experimentally, and thus reflects real working conditions. Rail vehicle and track irregularities model was not validated, but taken from the literature – as described later in text.

The proposed procedure for calculating the dynamic multi-domain co-simulation is as follows:

Step 1:

For the current input parameters and the adopted computational step, the MBD model of the pantograph and rail vehicle is solved. The equations of motion are solved using the Hilber-Hughes-Taylor integration scheme [21]. The calculations yield the current position of the pantograph slider head, which is then transferred to the FEM model of the catenary.

Step 2:

Then, for the same computational step, the FEM model of the catenary is solved by taking into account the current position of the pantograph slider head, as determined in the MBD model. The integration procedure used in the FE model is the Single-Step Houbolt scheme, which is unconditionally stable [21]. Next, number of iterations with frozen time are being computed to allow the two models (MBD and FEM) to agree on both force and displacement. Usually less than 10 iterations are needed for convergence. These calculations yield instantaneous CF acting on the contact wire of the catenary and the pantograph head.

Step 3:

The instantaneous value of the CF is then transmitted to the MBD model, which is solved for the next computational step, thus taking into consideration the subsequent positions of the rail vehicle and the pantograph resulting from the assumed vehicle speed and the size of the computational step.

Step 4:

Return to Step 2.

The steps for solving model equations described in points 2 and 3 are repeated in a loop for all the computational steps in the time interval used for analysis. In all the considerations presented in this work, the assumed simulation time corresponds to the travel of a rail vehicle along the 10 catenary spans (600 m), and the computational step is 0.001 s, similarly as proposed by Cho et al. [6].

3. Catenary FEM model

A very important phenomenon described in the literature, which influences the contact between the pantograph slider and the contact wire, is the propagation of the mechanical wave in the wires and its reflection from the rigid traction components. Therefore, the FEM is used for catenary model. The overhead contact line model used in the analysis corresponds to the model described in the EN 50318 [11]. The catenary has one contact wire and one messenger wire, nine droppers per span, and a single span length of 60 m. The height of the catenary is 1.2 m and the zig-zag stagger is ±0.2 m. The catenary model under consideration has been schematically represented in Figure 5.

The boundary conditions in the model reflect actual operating constrains that are present in real centenaries. The effect of gravity on traction components, the tensioning forces in the traction lines are considered as well. The wires in the catenary structure exhibit tensions of 16 kN (contact wire) and 20 kN (messenger wire). The linear density of cables is 1.07 kg/m and 1.35 kg/m respectively for the contact wire and the messenger wire. Due to the occurrence of staggering in zig-zag shape, the structure of the overhead contact line is modelled in
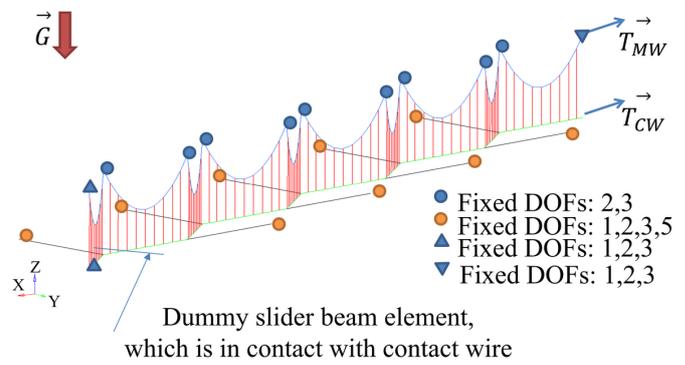

Fig. 5. The FEM model of a simple catenary system modelled as 3-D structure

three dimensions. According to the reference model description in the Standard, the catenary model does not take into account damping.

The diameter of wires is considerably smaller than their length, so the traction model uses 1D finite elements. These are type 98 elements (MSC.Marc solver) that take into account shear forces [22]. The model includes 100 elements per span for both the contact wire and the messenger wire. The assumed average length of the beam elements is 0.6 m. Such a size is considered small enough [28] and also allows to perform simulations efficiently.

The droppers exhibit nonlinear behaviour and they transmit tensile loads while remaining very loose during compression. To account for such bi-linear stiffness, elastic elements with nonlinear stiffness characteristics were used: 0 N/mm for compression and 100 N/mm for tension.

As shown in Figure 5, the rail vehicle and the pantograph move in a direction (-X). The position of the pantograph head, which is determined based on the MBD model, is related to the position of the dummy slider beam element modelled with the FEM model. This component is in contact with the contact wire. The contact algorithm used is the beam-to-beam contact which is available in MSC.Marc solver [21]. Contact is detected when the smallest distance between the dummy slider beam element and the contact wire is less than the assumed threshold value, i.e. 0.1 mm. The algorithm then automatically introduces a multipoint constraint equation to ensure that the elements do not interpenetrate. During the subsequent integration steps, the point of contact between the elements may change as the elements move relative to each other and stay in contact. In such a case, the multipoint constraint equation is automatically updated.

3.1. An initial configuration (pre-sag) of catenary

The pre-sag is an important parameter of the catenary which influences the dynamic interaction between the traction and the pantograph [7]. According to the adopted model of the catenary, the pre-sag is set to 0 mm. It is therefore necessary to adjust the length of the subsequent droppers to obtain zero pre-sag at the centre of the span under gravity and tension. The established procedure for determining the initial configuration of the catenary model has been schematically presented in Figure 6.

For the initially defined model (*Initial configuration, step 1*), we determine the difference between the required sag (0 mm) and the calculated sag value at the point of attaching droppers to the contact wire. Then, the model is reconfigured and the dropper lengths are corrected for the difference determined in the previous step (*initial configuration, step 2*). The procedure for static calculations and correction of droppers length is repeated until the sag value meets the requirements. To determine pre-sag, it was necessary to run nine iterations to adjust the droppers length, which were found as: 995.5; 813.8; 657.0; 563.0; 531.7 mm respectively for droppers counting from the end to the centre of a single span. Additionally, position of a fixed end of steady arms were found as translated from span ends by [0; 257.3; (+/-) 966.3] on X, Y and Z components respectively. Sign '+/-' for Z
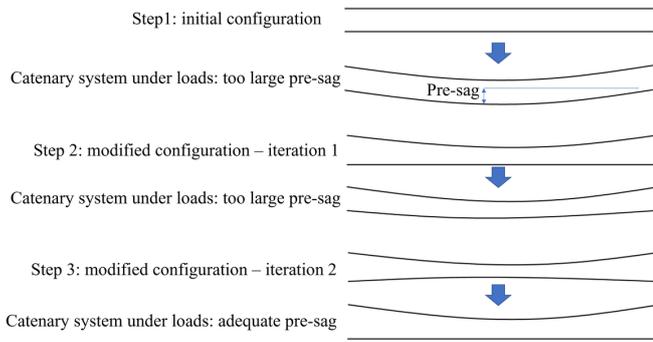
Fig. 6. Iterative procedure for determining catenary state under initial loads

translation corresponds to zig-zag shape for subsequent spans. Resulting pre-sag error for designed model of the catenary is less or equal 0.13 mm.

3.2. Catenary model validation

The subsequent step of the work included validation of the numerical model. The standard solution consists of performing experiments and comparing the results obtained for the CF course and the contact wire uplift with the numerical model. This can only be done by measuring CF indirectly, and is expensive and difficult. During our work, we validated the numerical model based on basic validation procedure described in the EN 50318. The process of validation of the numerical model consists of comparing statistical parameters describing the course of CF and contact wire lift with the tolerances given in this standard for precisely described catenary model. The standard utilizes basic pantograph model with lumped parameters and two degrees of freedom. Detailed information on the pantograph model can be found in the previously referenced standard. The validation procedure requires the statistical parameters of CF and contact wire uplift to be determined. The results are then compared with the allowable limits given by that standard. Simulation were performed for passage speed 250 km/h and 300 km/h. Please note that the computed statistical parameters are determined for a limited amount of data, i.e., for the two central spans of the catenary. Such an approach aims to exclude the impact of the boundary conditions on the results obtained. In case of CF results, they are filtered using a low-pass filter with a cut-off frequency of 20 Hz. Figure 7 presents results obtained in computer simulations for 250 km/h passage speed, but similar results were obtained also for passage speed 300 km/h. Results of uplift of contact wire at steady arms' location are presented in Figure 7A, while Figure 7B depict simulated CF in pantograph-catenary interface. Vertical lines in both figures depict section of two central spans of catenary. The integration time steps in both cases (250 and 300 km/h) were the same and set to 0.001 s.

Statistical parameters of the CF and wire uplift courses are computed next. The results are provided in Table 1. It can be noted that all parameters are within the acceptance ranges for both analysed passage speeds. Therefore, the obtained results successfully validated the numerical model according to the adopted methodology described in the Standard. It can be concluded that the formulated catenary model reflects the real dynamic behaviour of the catenary with deviations accepted by the standard.

4. Pantograph and rail vehicle model

The validity of the pantograph model is very important for the representation of the realistic interaction with catenary. Important factors affecting how the pantograph cooperates with the catenary, which are taken into account in the model developed here, include the vibrations of the railway vehicle that are transmitted to the pantograph frame, the influence of electromagnetic and aerodynamic forces on the pan-

tograph components, energy dissipation through friction in the kinematic joints of the pantograph, and the actual spatial structure of the pantograph kinematic chain.

The model of the pantograph mechanism was formulated using the MBD method. With this method the number of degrees of freedom can be reduced compared to the FEM model, making the MBD model computationally efficient. At the same time, this modelling method allows for the implementation of forces resulting from all the relevant phenomena that affect the pantograph components. The model was formulated using the MSC.Adams package. For the formulation of the MBD model, it is necessary to define spatial configuration of the pantograph components and joints between them. The developed pantograph model is shown in Figure 8.
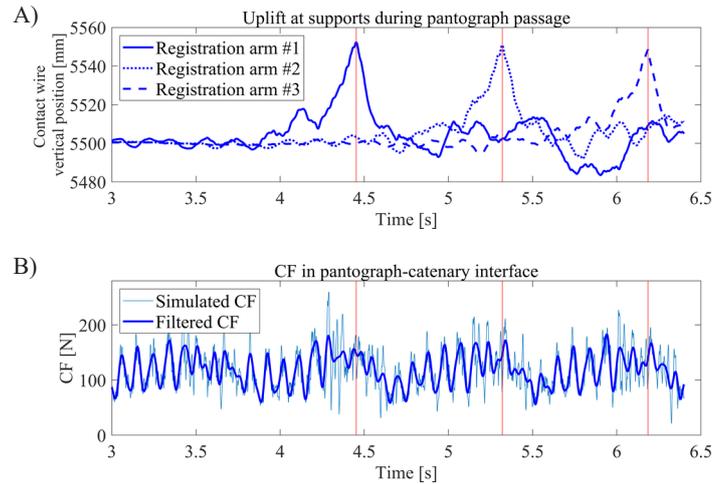

Fig. 7. Results of computed contact wire uplift (A) and CF (B) in case of 250 km/h train speed
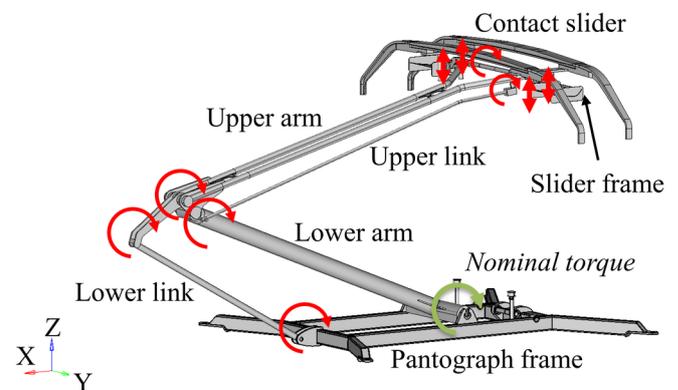

Fig. 8. Scheme of pantograph MBD model

All the modelled pantograph components are marked in the scheme. Their mass and moment of inertia parameters are taken from the manufacturer's technical documentation. There are rotational kinematic pairs between the components marked with circular arrows. In addition, in the place where the revolute joint is found between *the pantograph frame* and *lower arm* components torque forcing applies from the pantograph pneumatic drive (*Nominal torque*). Linear arrows show the locations of the pantograph head suspension springs in the model. The stiffness and damping parameters of the slider suspension are fundamental in determining the quality of cooperating with the catenary. Thus, experimental testing was necessary to identify the characteristics of the slider suspension for the utilized 160ECT pantograph. The results of performed experiments are presented in our recent paper [34]. Experimentally determined stiffness and damp-

Table 1. Catenary model validation results

Parameters		Simulation results	Accepted ranges	Simulation results	Accepted ranges
Speed [km/h]		250	250	300	300
Mean CF [N] F_M		117.7	110-120	117.9	110-120
Standard deviation of CF [N] σ		28.17	26-31	36.3	32-40
Statistical maximum of CF: $F_M+3\sigma$		202.21	190-210	226.8	210-230
Statistical minimum of CF: $F_M-3\sigma$		33.19	20-40	9	(−5)-20
Actual maximum of CF [N]		182.5	175-210	205.5	190-225
Actual minimum of CF [N]		56.63	50-75	33.6	30-55
Maximum uplift at supports [mm]	Support 1	52.4	48-55	57.2	55-65
	Support 2	51		60.1	
	Support 3	48.4		60.7	
Percentage contact loss [%]		0	0	0	0

ing properties of slider suspension are implemented next in the numerical model as lumped parameters elements (K=3.93 N/mm and C=0.0005 Ns/mm).

The pantograph system dissipates some amount of energy thanks to the friction torque that is present in kinematic pairs. Our recently presented study [35] made it possible to fine-tune the dry friction coefficients in the revolute joints to reflect the experimentally determined characteristics of energy dissipation by friction in joints of the pantograph.

The dynamics of the rail vehicle is also an important factor influencing the interaction of the pantograph with the catenary. A rail vehicle with two-level suspension with two bogies and eight wheels was taken into account in our model. The scheme of the model has been presented in Figure 9.

The parameters of the rail vehicle model are taken from the work by Zboiński et al. [33]. The rail vehicle moves in the negative direc-

Fig. 9. Scheme for a rail vehicle model

tion relative to the global X direction at a pre-defined speed. During the run, the vehicle wheels are subjected to vertical track irregularities. With a model formulated in this way, it is possible to take into account vibrations of the rail vehicle body. In turn, those vibrations affect the pantograph frame, and therefore influence the current collection quality.

In reality, there are also lateral track's profile irregularities, but in this study we consider only vertical ones, since they are of the greatest importance when driving on straight-line sections of tracks (and such a section is simulated). The track vertical irregularities profile has been generated based on the methodology published in the work by Karttunen et al. [16]. The authors presented formula that allows to describe irregularities as a random data characterized by the following expression for the power spectral density (PSD) in spatial form:

$$S_A(\lambda) = 2\pi \frac{A_A \cdot \Omega_c^2}{\left(\left(\frac{2\pi}{\lambda}\right)^2 + \Omega_r^2\right)\left(\left(\frac{2\pi}{\lambda}\right)^2 + \Omega_c^2\right)} \quad (1)$$

where $\Omega_c = 0.82$ rad/m, $\Omega_r = 0.02$ rad/m are pre-set cut-off frequencies and λ is the wavelength in [m], wavelengths are taken in range of 3-150 m, and a number of 500 waveforms were used to generate realistic profiles. The parameter A_A [m·rad] corresponds to the amplitude of irregularities and the utilized value of $4.1 \cdot 10^{-7}$ represents a medium quality track. To obtain the track irregularities profile in sense of a distance function, the PSD formula is retransformed using the inverse Fourier transform with random phases. Importantly, the courses obtained are characterized by randomness, while their statistical parameters meet the criteria for the middle class of track quality.

In the considerations presented in this work, we have computed the individual track profiles for the right and left rails separately. The vertical irregularities generated using above mentioned procedure and implemented in the multi-domain model are shown in Figure 10.

4.1. Aerodynamic and electromagnetic induction forces

Aerodynamic forces are one of the external forces loading pantograph components. Especially at high speeds they influence the dynamic interaction between pantograph and catenary. The current standard for railway applications describes acceptable average CF ranges for different train speeds, including the aerodynamic effects on pantograph [12]. Dai et al. [8] in their recent research investigated the influence of additional baffles application in the pantograph head. The goal was to tune the aerodynamic lift force on the pantograph components, which influences the CF mean value. Thanks to the great influence of aerodynamic forces, the multi-domain model
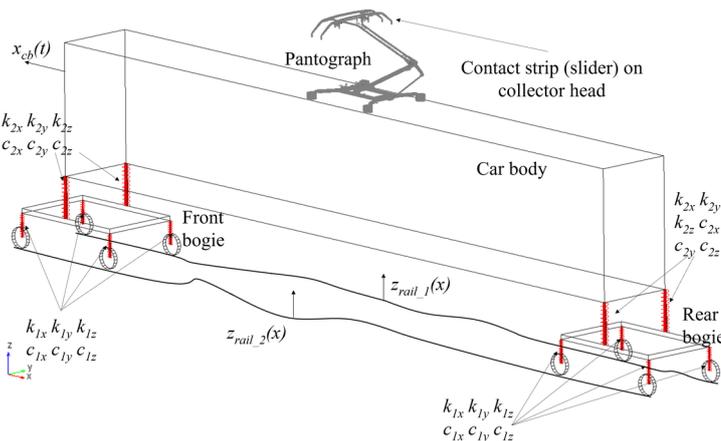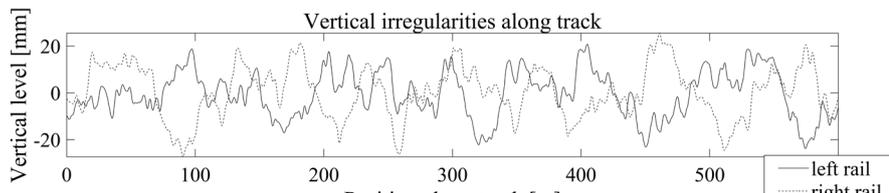
Fig. 10. Utilized vertical tracks' profile

utilised in this paper has to include this phenomenon. Aerodynamic properties for the adopted pantograph model were investigated in our recent paper [36]. In general, the numerical model which employs the Fluid-Structure-Interaction method has been formulated first. Individual aerodynamic forces which load all components of the pantograph were computed then using Altair AcuSolve solver. Next, forces were implemented into the MBD pantograph model, and then the resulting uplift force exerted by the pantograph head on the contact wire was computed. Experimental tests were performed in the wind tunnel as well, for numerical model validation. The key results of this research are presented in Table 2.

The results obtained for the numerical model and in the experiment showed a high agreement (relative error up to 2%),

Table 2. Uplift force under aerodynamic forces

Uplift force	Air flow speed [km/h]		
	120	140	160
Experiment [N]	124.2	129.4	135.4
Numerical model [N]	122.2	128.9	135.4
Relative error	2%	0.4%	0.4%

which prove positive numerical model validation. It should be noted that, in fact, the pantograph moves at a certain speed and thus makes the surrounding air to flow around it. In the conducted numerical analyses and tests in the wind tunnel, the opposite situation was assumed: the stationary pantograph interacted with a forced stream of air at a given velocity. Such a simplification is used in practice, such as in ref. [8], in order to limit the number of factors influencing the uplift force. Indeed, the aim of the research was to determine only the influence of aerodynamics - with omission of other factors, which is impossible during the actual journey of the vehicle. In order to best reflect the operating conditions of the pantograph, the experimental tests were carried out in a wind tunnel with an open measurement space. Thanks to it the impact of disturbed flow in the boundary layer of wind tunnel was minimized. In the numerical analysis, care was taken to ensure that the model reflects the pantograph on the wind tunnel test stand as accurately as possible.

The electromagnetic force is another potentially important phenomenon taken into account in the multi-domain model of the dynamic interaction between the pantograph and the catenary. According to Liu et al. [19] inclusion of electromagnetic force is one of the directions of the pantograph-catenary models development. In fact the pantograph head through which electric current flows, is located in the magnetic field inducted around the contact wire, as shown schematically in Figure 11.

Considering the above presented assumptions, the pantograph head is affected by the electromagnetic force. The computational model proposed was presented in the work by Zdziebko et al. [37]. For the assumed current load scenario of the contact wire |PRC"ST| the computation rule is as follows. Using Biot-Savart law, the magnetic induction vector is determined at the subsequent points of the pantograph slider head |AB| from individual contact wire pieces |PR|, |RC"|, |C"S|, and |ST|. Then, for the assumed current flow distribution in slider head segments |AC| and |CB|, the electromagnetic force acting on each of

its segments, with an assumed finite length, is calculated. The resultant electromagnetic force acting on is calculated as the sum of the forces acting on all segments in each direction. Based on the simulations conducted, we demonstrated that, depending on the working height of the pantograph, electromagnetic force influence may results in an increase of the static uplift force by 2N (Figure 12).
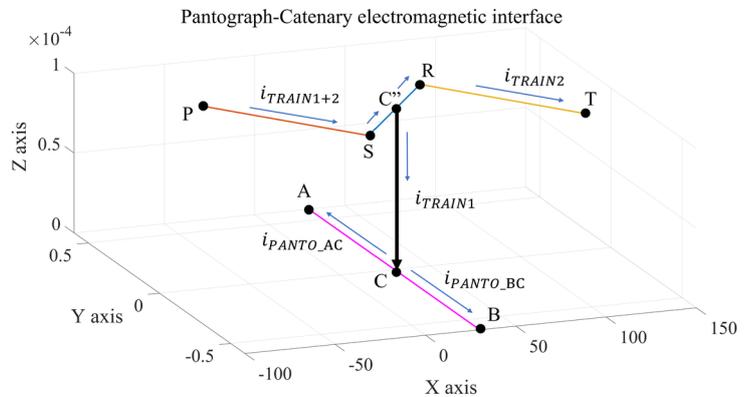

Fig. 11. Scheme of electricity flow in adopted scenario (axis units in [m])
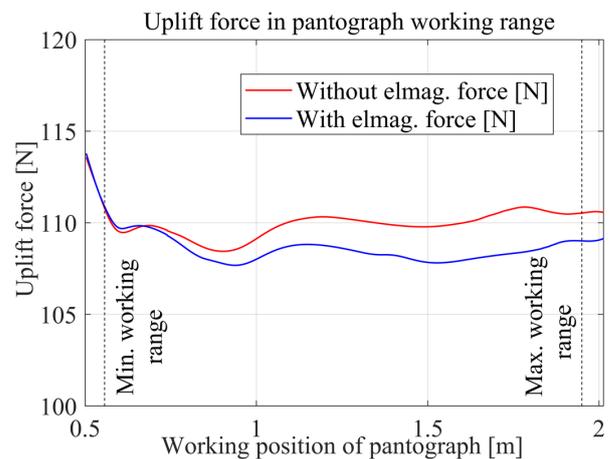

Fig. 12. Influence of electromagnetic force on uplift force for various pantograph working heights

The received results show, that the influence of electromagnetic force on uplift force depends on working height of the pantograph, but is significantly lower than influence of aerodynamic forces.

5. Results of multi-domain simulations

Hereafter we present the results of numerical simulations employing the multi-domain model described in Sections 2 to 4. The computation time for simulating the interaction between the pantograph and the catenary over a 600 m-long section is about 70 minutes. Simulations were performed using an available workstation with the following configuration: CPU Intel R Core™ i7-2600K 3.4GHz x64, 32GB RAM, 1TB HDD.

Results of computed CF for driving speed of 160 km/h is shown in Figure 13A. The analysis of statistical parameters describing variations in the course of the CF was limited to two central spans and was filtered as described in Section 3.2 (Figure 13B). The 160ECT pantograph is certified to a maximum speed of 160 km/h, but for testing purposes, numerical simulations were performed in an extended speed range of 120–200 km/h. The statistical parameters usually em-
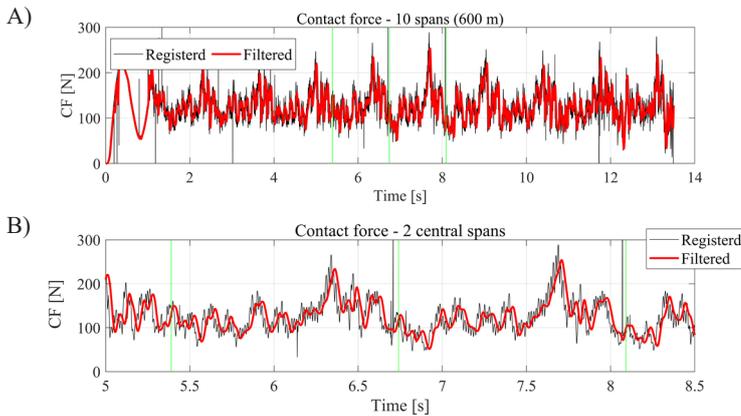
A)

B)

Fig. 13. CF time history computed for 600 m distance (A) and close-up view for the two central spans (B) – vertical lines depict two central spans

ployed to determine the pantograph-catenary interaction quality are shown in Table 3.

Table 3. The results of pantograph-catenary dynamic interaction computed with complex multi-domain model, after low-pass filtration

Rail vehicle speed [km/h]:	120	160	200
Mean CF [N]:	118.4	131.7	132.9
STD of CF [N]:	17.3	38.6	59.6
Min. of CF[N]	82.3	37.2	-3.7 (0N)
Max. of CF[N]	173.2	260.3	290.9
Peak-to-Peak of CF [N]:	90.9	223.1	294.5

The results obtained show that for a train speed of 120 km/h the mean uplift force is much lower than the corresponding value obtained for the higher driving speeds. This is due to aerodynamic forces being significantly reduced when driving at low speed. For higher speeds, the CF exhibits more varied behaviour expressed by relatively higher STD and peak-to-peak CF parameters. At a speed of 200 km/h, detachments of contact strip from the contact wire were observed. In the originally computed CF time history, the value of 0N was recorded while detachments. Nevertheless, the course of CF after filtration was statistically analysed (Table 3), therefore the presented value of Min. of CF is below zero - it is caused by the effect of low-pass filtration.

At a subsequent stage of our work, we investigated the CF in the pantograph-catenary system as well as its change resulting from the choice on the analysed physical phenomena distorting the force interaction in the mentioned system. The analysis consisted of observing selected statistical parameters of the CF in different computational cases where the presence of individual sub-models related to a given physical phenomenon was either ignored or taken into account. The results are presented in Figure 14. The case in which all phenomena described earlier and the corresponding computational models were taken into account was considered as a reference – this case is marked with 'X'. The calculation for the full model resulted in the CF course described by the following statistical parameters: Mean CF of 131.7 N and CF STD of 38.6 N. The analysis was limited only to these statistical parameters and to a single-speed value of 160 km/h.

The simulation results show that the inclusion of aerodynamic forces has the greatest impact on the change in mean CF. The aerodynamic forces exclusion causes the mean CF to decrease approximately by 25 N. On the other hand, small effects of the presence of electromagnetic force on the results obtained have also been noticed. Its omission does not significantly change the results obtained (change in CF STD of 0.6 N and change in mean CF of 1.9 N). If the multi-domain model ignores phenomena associated with the non-linear behaviour of the

droppers or friction in kinematic pairs, the STD of CF increases by 7.5 N and 8.4 N respectively. In addition, excluding the track irregularities from the model results in lowering the STD of CF by 4 N compared to the comprehensive multi-domain model, while the mean CF remains at a similar level. Our analysis shows that aerodynamic forces must be included in the model of dynamic interaction between the pantograph and the catenary. Moreover, it is recommended to include a model of non-linear droppers, friction in the pantograph joints, and the dynamics of the rail vehicle and track irregularities. These factors have a significant effect on the change in CF STD, but their impact on the mean CF is negligible. However, electrodynamic forces may be omitted from modelling as they only negligibly affect the results obtained. This applies to the mean CF and CF STD alike.
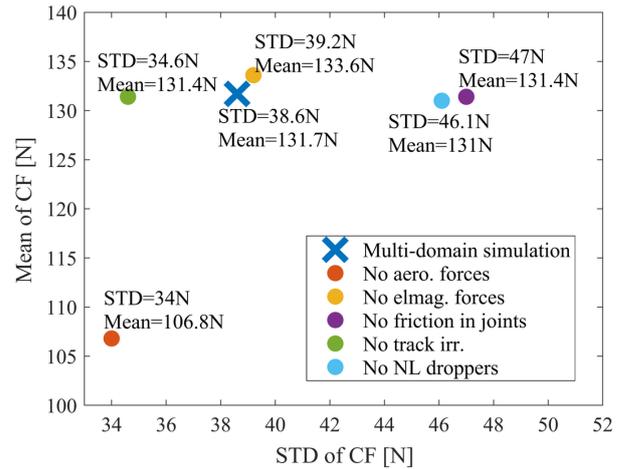

Fig. 14. Influence of physical phenomena exclusion in model on the obtained CF results

6. Summary and concluding remarks

The development of computer simulation techniques dedicated to the pantograph-catenary system is still open to discussion. This system is subjected to several physical phenomena which significantly affect the resulting interaction of the pantograph with the catenary. Computer-aided numerical tools are very helpful when designing new system components and it is necessary to develop them to reflect as accurately as possible the actual operating conditions of the system under analysis. The computational methodology presented in this work allows for the formulation of a multi-domain model, which in turn allows for the analysis of the effects of these phenomena on the dynamics of the pantograph-overhead contact line system. From the literature review presented in the introduction, it can be concluded that such a comprehensive multi-domain model for simulating the dynamic interaction between the pantograph and the catenary has not yet been published. The numerical model proposed hereby states a comprehensive methodology for pantograph-catenary simulations. Together with the inclusion of such phenomena as vibrations from the rail vehicle, the effects of electromagnetic and aerodynamic forces, the propagation of the mechanical wave in the catenary, the actual kinematic chain of the pantograph, together with the friction model in joints and the suspension model of the pantograph (3D) makes the approach to be innovative. The model accounts for strong non-linearity: the contact of the slider and the catenary and the non-linear characteristics of droppers.

The analysis of physical phenomena accounted for in the multi-domain model shows that the model of aerodynamic influence is very significant as it greatly affects the change in the mean CF and CF STD compared to the nominal case. It is also recommended to take into account the model of non-linear droppers, friction in the panto-

graph joints, the dynamics of the rail vehicle, and track irregularities. Omission of these factors cause the CF STD to change significantly, but no significant change in the mean CF is observed. The impact of electromagnetic force has negligible effect on the results of pantograph-catenary dynamic interaction and thus may be omitted in the modelling process.

Further directions of work are related to development of the computational model with the friction between the slider and the contact wire of the catenary. So far it has not been included in the model and it is potentially an important factor, which may influence the interaction of the pantograph with the catenary. Moreover, development of other traction system (DC/AC) models might be an interesting challenge for multi-system pantographs simulations.

References

1. Ambrósio J, Rauter F, Pombo J, Pereira M. Co-Simulation Procedure for the Finite Element and Flexible Multibody Dynamic Analysis. 11th Pan-American Congress of Applied Mechanics, January 04-08, 2010, Foz do Iguacu, PR Brasil, 2010.
2. Ambrósio J, Rauter F, Pombo J, Pereira MS. A Flexible Multibody Pantograph Model for the Analysis of the Catenary-Pantograph Contact. In Arczewski K, Blajer W, Frączek J, Wojtyra M (eds): Multibody Dynamics Computational Methods and Applications, Springer: 2011; 23: 1-27, https://doi.org/10.1007/978-90-481-9971-6_1.
3. Bucca G, Collina A. A procedure for the wear prediction of collector strip and contact wire in pantograph-catenary system. Wear 2009; 266(1-2): 46-59, https://doi.org/10.1016/j.wear.2008.05.006.
4. Carnicero A, Jimenez-Octavio JR, Such M et al. Influence of static and dynamics on high performance catenary designs. International Conference on Pantograph Catenary Interaction Framework for Intelligent Control - PACIFIC 2011. Amiens, Francia. 8 Diciembre 2011, 2011.
5. Chen GX, Yang HJ, Zhang WH et al. Experimental study on arc ablation occurring in a contact strip rubbing against a contact wire with electrical current. Tribology International 2013; 61: 88-94, https://doi.org/10.1016/j.triboint.2012.11.020.
6. Cho YH. Numerical simulation of the dynamic responses of railway overhead contact lines to a moving pantograph, considering a nonlinear dropper. Journal of Sound and Vibration 2008; 315(3): 433-454, https://doi.org/10.1016/j.jsv.2008.02.024.
7. Cho YH, Lee K, Park Y et al. Influence of contact wire pre-sag on the dynamics of pantograph-railway catenary. International Journal of Mechanical Sciences 2010; 52(11): 1471-1490, https://doi.org/10.1016/j.ijmecsci.2010.04.002.
8. Dai Z, Li T, Zhou N et al. Numerical simulation and optimization of aerodynamic uplift force of a high-speed pantograph. Railway Engineering Science 2021, https://doi.org/10.1007/s40534-021-00258-7.
9. Ding T, Chen GX, Bu J, Zhang WH. Effect of temperature and arc discharge on friction and wear behaviours of carbon strip/copper contact wire in pantograph-catenary systems. Wear 2011; 271(9): 1629-1636, https://doi.org/10.1016/j.wear.2010.12.031.
10. EC Engineering. Internal report: Pantograph 160ECT. 2016.
11. European Committee for Electrotechnical Standardization EN-50318:2002. Railway applications - Current collection systems. Validation of simulation of the dynamic interaction between pantograph and overhead contact line. 2002.
12. European Committee for Electrotechnical Standardization EN-50367:2012. Railway applications - Current collection systems - Technical criteria for the interaction between pantograph and overhead line). 2012.
13. Grajnert J. Zastosowanie tłumienia w odbieraku prądu. Pojazdy Szynowe 1977.
14. Grajnert J, Marcinkowski J. Zwis wstępny przewodu jezdnego jako czynnik eksploatacyjny kształtowania dynamiki współpracy odbieraka prądu z siecią trakcyjną. Trakcja i Wagony 1982.
15. Jiménez-Octavio JR, Such M, Carnicero A, Lopez-Garcia O. Validation of Simulation Approaches for Catenary-Pantograph Dynamics. Civil-Comp Proceedings 2008; 88: 1-11.
16. Karttunen K, Kabo E, Ekberg A. The influence of track geometry irregularities on rolling contact fatigue. Wear 2014; 314(1-2): 78-86, https://doi.org/10.1016/j.wear.2013.11.039.
17. Lewandowski J, Młynarski S, Pilch R et al. An evaluation method of preventive renewal strategies of railway vehicles selected parts. Eksploatacja i Niezawodnosc – Maintenance and Reliability 2021; 23(4): 678-684, https://doi.org/10.17531/ein.2021.4.10.
18. Liu Z, Jönsson PA, Stichel S, Rønnquist A. Implications of the operation of multiple pantographs on the soft catenary systems in Sweden. Proceedings of the Institution of Mechanical Engineers, Part F: Journal of Rail and Rapid Transit 2016; 230(3): 971-983, https://doi.org/10.1177/0954409714559317.
19. Liu Z, Song Y, Han Y et al. Advances of research on high-speed railway catenary. Journal of Modern Transportation 2018; 26(1): 1-23, https://doi.org/10.1007/s40534-017-0148-4.
20. Massat JP, Laurent C, Bianchi JP, Balmès E. Pantograph catenary dynamic optimisation based on advanced multibody and finite element co-simulation tools. Vehicle System Dynamics 2014; 52(SUPPL. 1): 338-354, https://doi.org/10.1080/00423114.2014.898780.
21. MSC.Software. Marc Volume A: Theory and User information. 2016.
22. MSC.Software. Marc Volume B: Element library. 2016.
23. Nagasawa H, Kato K. Wear mechanism of copper alloy wire sliding against iron-base strip under electric current. Wear 1998; 216(2): 179-183, https://doi.org/10.1016/S0043-1648(97)00162-2.
24. Oz MA, Kaymakcı OT, Koyun A. A safety related perspective for the power supply systems in railway industry. Eksploatacja i Niezawodnosc – Maintenance and Reliability 2017; 19(1): 114-120, https://doi.org/10.17531/ein.2017.1.16.
25. Pappalardo CM, Patel MD, Tinsley B, Shabana AA. Contact force control In multibody pantograph/catenary systems. Proceedings of the Institution of Mechanical Engineers, Part K: Journal of Multi-body Dynamics 2016; 230(4): 307-328, https://doi.org/10.1177/1464419315604756.
26. Park TJ, Han CS, Jang JH. Dynamic sensitivity analysis for the pantograph of a high-speed rail vehicle. Journal of Sound and Vibration 2003; 266(2): 235-260, https://doi.org/10.1016/S0022-460X(02)01280-4.

27. Pombo J, Ambrósio J, Ambrosio J. Environmental and track perturbations on multiple pantograph interaction with catenaries in high-speed trains. Computers and Structures 2013; 124: 88-101, https://doi.org/10.1016/j.compstruc.2013.01.015.
28. Sanchez-Rebollo C, Jimenez-Octavio JR, Carnicero A. Active control strategy on a catenary-pantograph validated model. Vehicle System Dynamics 2013; 51(4): 554-569, https://doi.org/10.1080/00423114.2013.764455.
29. Song Y, Ouyang H, Liu Z et al. Active control of contact force for high-speed railway pantograph-catenary based on multi-body pantograph model. Mechanism and Machine Theory 2017; 115: 35-59, https://doi.org/10.1016/j.mechmachtheory.2017.04.014.
30. Song Y, Wang Z, Liu Z, Wang R. A spatial coupling model to study dynamic performance of pantograph-catenary with vehicle-track excitation. Mechanical Systems and Signal Processing 2021; 151: 107336, https://doi.org/10.1016/j.ymssp.2020.107336.
31. Wu TX, Brennan MJ. Dynamic stiffness of a railway overhead wire system and its effect on pantograph-catenary system dynamics. Journal of Sound and Vibration 1999; 219(3): 483-502, https://doi.org/10.1006/jsvi.1998.1869.
32. Wu TX, Brennan MJ. Basic analytical study of pantograph-catenary system dynamics. Vehicle System Dynamics 1998; 30(6): 443-456, https://doi.org/10.1080/00423119808969460.
33. Zboiński K, Dusza M. Bifurcation analysis of 4-axle rail vehicle models in a curved track. Nonlinear Dynamics 2017; 89: 863-885, https://doi.org/10.1007/s11071-017-3489-y.
34. Zdziebko P, Martowicz A, Uhl T. Experimental and numerical investigation on the components of a pantograph slider suspension. MATEC Web Conf. 2019, https://doi.org/10.1051/matecconf/201925205003.
35. Zdziebko P, Martowicz A, Uhl T. An investigation on the influence of pantograph friction on its interaction with a catenary using co-simulations. Proceedings of ISMA 2018 - International Conference on Noise and Vibration Engineering and USD 2018 - International Conference on Uncertainty in Structural Dynamics, Katholieke Univ Leuven, Dept Werktuigkunde: 2018: 3283-3294.
36. Zdziebko P, Martowicz A, Uhl T. An investigation on the active control strategy for a high-speed pantograph using co-simulations. Proceedings of the Institution of Mechanical Engineers, Part I: Journal of Systems and Control Engineering 2018: 095965181878364, https://doi.org/10.1177/0959651818783645.
37. Zdziebko P, Martowicz A, Uhl T. An investigation into multi-domain simulation for a pantograph-catenary system. ITM Web of Conferences 2017; 15: 03001, https://doi.org/10.1051/itmconf/20171503001.